Dissertations, Master's Theses and Master's Reports - Open

Dissertations, Master's Theses and Master's Reports

2014

Skin Lesion Extraction And Its Application

Yanliang Gu
Michigan Technological University

SKIN LESION EXTRACTION AND ITS APPLICATION

By

Yanliang Gu

A THESIS

Submitted in partial fulfillment of the requirements for the degree of

MASTER OF SCIENCE

In Medical Informatics

MICHIGAN TECHNOLOGICAL UNIVERSITY

2014

This thesis has been approved in partial fulfillment of the requirements for the Degree of MASTER OF SCIENCE in Medical Informatics.

School of Technology

Thesis Advisor: *Jinshan Tang*

Committee Member: *Guy Hembroff*

Committee Member: *Guiliang Tang*

School Dean: *James Frendewey*

Table of Contents

List of Figures

List of Tables

Acknowledgements

First and foremost, I would like to thank my advisor, Dr. Jinshan Tang, for encouraging me to explore my interests rather than simply handing me a thesis topic. His guidance and instruction were invaluable, and this experience has been far more enriching than I ever imagined. I would also like to thank my family and friends for their support and especially for those times when they dragged me away from the office for a much-needed break. I could not have completed this work without their support.

Abstract

In this thesis, I study skin lesion detection and its applications to skin cancer diagnosis. A skin lesion detection algorithm is proposed. The proposed algorithm is based color information and threshold. For the proposed algorithm, several color spaces are studied and the detection results are compared. Experimental results show that YUV color space can achieve the best performance. Besides, I develop a distance histogram based threshold selection method and the method is proven to be better than other adaptive threshold selection methods for color detection. Besides the detection algorithms, I also investigate GPU speed-up techniques for skin lesion extraction and the results show that GPU has potential applications in speeding-up skin lesion extraction. Based on the skin lesion detection algorithms proposed, I developed a mobile-based skin cancer diagnosis application. In this application, the user with an iPhone installed with the proposed application can use the iPhone as a diagnosis tool to find the potential skin lesions in a persons' skin and compare the skin lesions detected by the iPhone with the skin lesions stored in a database in a remote server.

Chapter 1. Background

1.1. skin cancer

Cancer is one of the biggest threats to human beings and is the second leading cause of death the entire world human [1]. According to the statistical data from WHO(World Health Organization) [2], cancer caused about 7.6 million people death worldwide in 2008, and it is predicted that the number of deaths caused by cancer is being increased and   the number will possibly increase to 13.1 million in 2030 [2]. Based on related research, cancer will become the leading death in next 20 years [3].

Of all the known cancers, in USA, skin cancer is the most prevalent form of cancer [4]. It is found that each year, more new cases of skin cancer are diagnosed than all the cases of breast cancers, prostate cancers, lung cancers, and colon cancers diagnosed [5]. Based on the statistics in 2008, in USA about 6,000 people were diagnosed with melanomas of the skin, and more than 8,000 people died from it [6]. In Americans lifetime, one in five of them will develop skin cancer [7].

There are three types of skin cancer: Basal cell cancer and squamous cell cancer are called non-melanoma skin cancer while melanoma is on melanocytes cells, Basal

cell cancer and squamous cell cancer are common but less dangerous. Melanoma is not common as non-melanoma skin cancers, however, it is more likely to spread and become fatal [8].

Although skin cancer is a threat to human life, fortunately even melanoma can be cured if it is detected early. According to research, the curable rate will be more than 90% high if cancer can be diagnosed in its early stages while the curable rate will be less than 50% in its late stage [9]. Thus, the detection of skin cancer in its early stage has attracted the attention from different fields [10].

Currently the diagnosis of skin cancer is done mainly by a human, who is called dermatologist. During diagnosis, a dermatologist exams the skin carefully by his eyes or using a device called dermascope. During this stage, dermatologists generally use "ABCD" rule to find the signs of skin cancer [11]. ABCD means Asymmetry, Borders (irregular), Color (variegated), Diameter (greater than 6mm) of a skin patch [11]. By observing the early signs using "ABCD" rule, dermatologists can classify whether a skin patch is benign or malignant. If a patch is determined to be malignant, a biopsy will be used to confirm the final result [12]. Although the procedure used above is standard, a dermatologist has subjective bias and the correct

diagnosis depends on a dermatologist's experience. Besides, the procedure examined by a dermatologist takes long time. In order to improve the diagnosis rate, computer aided skin cancer detection techniques have been investigated to aid the dermatologists for skin cancer detection. The basic idea of computer-aided detection (CAD) is to use imaging technique, image processing technique, and pattern recognition technique to detect the suspected skin patches. It is used generally as the second opinion to a dermatologist.

In this thesis, I mainly study the key technique used in CAD system for skin cancer detection. The key technique is the extraction of the boundary of skin lesions. Two algorithms for the extraction of the boundary of skin lesions are proposed. Besides, I also develop an application based on iPhone which can be used for skin cancer detection by a person which is not a dermatologist. The iPhone based skin cancer detection application provide a care-everywhere tools which provide a good skin care method potentially and help a person find skin cancer possibly without going to a clinic.

1.2.　Skin lesion detection with CAD

The development of CAD systems and related techniques have been over 20 years and many systems have been developed [13]. In [14], a skin cancer detection system was developed by F. Ercal. In the proposed system, the border of the skin lesion was extracted by doctors and the features were constructed using ABCDE rule. A commercial neural network classifier was adopted to classify the skin lesions into benign or malignant. This system can achieve 80% accuracy rate. In [15], another computer program named MoleSence was developed by Opticom Data Research. This program also used "ABCDE rule" to analyze the skin cancer images. In [16], an automated melanoma recognition system was developed by H. Ganster. In the system, automated image segmentation was accomplished by fusing the output of 3 algorithms and the segmentation accuracy is 96%. A 24-NN (Nearest Neighbor) classifier was used for skin cancer classification and it achieved 73% melanoma recognition rate. The sensitivity and specificity are 87% and 92% for the "not benign" class in a two class scenario. In [17], Handyscope was developed by the company called Fotofinderin Germany. It merges a dermatoscope with an iPhone and can extract lesion features. However, it does not incorporate lesion classification in the same device.

In all of the CAD systems described above, one key technique is to extract the lesion

region from the background and thus it has attracted a lot of efforts. Two widely used techniques are thresholding and region growing. Both of the two techniques can achieve good performance for boundary extraction when the boundaries of skin lesion images are clear. However, the techniques will fail if the boundary of the lesion region is unclear. For the images with unclear boundaries, many algorithms have been developed. A multi-direction gradient vector flow (GVF) is proposed for skin cancer border extraction in [18]. In the proposed method, a new anisotropic diffusion filter employing new gradient computation and adaptive threshold selection method was used to remove the noise. After noise reduction, the system used a multi-direction GVF snake which was extended from the single direction GVF snake to segment the skin cancer image [18]. In [19], an automatic detection method employing radial search algorithm to detect irregular borders in skin tumor images was proposed. In [20], a method based on domain-specific algorithms was used to extract the boundary of skin lesion, and this method can achieve high success rate. In [21], an automatic approach for skin cancer segmentation was proposed by the modification of Region-based Active Contour model (RACM). In the proposed approach, initial threshold was set automatically and a function named Courant-Friedreichs-Lewy (CFL) was used to enforce the stability of curves. Compared with other state-of-the-art methods, this approach achieves a better

accuracy. From [22], a method based on a principle components transform algorithm was developed for automatic color segmentation. This method could detect the borders of skin cancer in six different color spaces. Many images were obtained with low contrast and lack color calibration, thus in [23], an approach to improve the accuracy of skin cancer segmentation for these cases was provided. This approach enhanced color information by a pre-processing step and then skin cancer segmentation was performed on the pre-processed images. In [24], a segmentation algorithm based on an evolution strategy (EV) was provided to detect the skin cancer area. The segmentation results were compared with those obtained by a dermatologist and the comparison showed that the proposed method can get high accuracy for images with high-level noise. Using region fusion and narrow band energy graph partitioning technology, a novel multi-modal skin lesion segmentation method was developed in [25]. The proposed method can process skin cancer images with blurred and irregular edges well and can achieve a better performance compared with other state-of-the-art segmentation methods. A new automatic skin cancer segmentation method was introduced in [26]. The method first converted a color image into a gray image and then the image is segmented using intensity thresholding. The segmentation is refined using image edges.

Although many boundary extraction algorithms have been proposed, the existing

algorithm is still far from real application and thus thesis will attack this difficult.

1.3. Statement of Problem

The aim of this thesis is to investigate new boundary extraction algorithms. The proposed algorithm is based color information and threshoding. In the proposed algorithm, the key problem is how to select color space and threshold. I compared different color spaces and find the best one. For threshold selection, I developed a distance histogram based algorithm which can achieve much better performance than traditional thresholding algorithm. Besides, I developed a mobile-based skin cancer diagnosis application. In this application, the user with an iPhone installed with the proposed application can use the iPhone as a diagnosis tool to find the potential skin lesions in a persons' skin and compare the skin lesions detected by the iPhone with the skin lesions stored in a database in a remote server. In the iPhone applications, the key step is to compare the similarity between two boundaries. Fourier descriptor is investigated in the thesis.

The rest of the thesis is organized as follows. In Chapter 2, I introduce some basic knowledge of color modeling and noise reduction. Then I investigate my new segmentation method and discuss different color modeling methods and different

noise reduction methods. I also introduce GPU techniques for skin lesion extraction and the results show that GPU has potential applications in skin lesion extraction. In Chapter 3, I develop an IPhone application for skin lesion image retrieval. In Chapter 4, I conclude the Thesis.

Chapter 2. Skin Lesion Extraction Based on Color Information and Thesholding

2.1. General Framework

My skin lesion segmentation system consists of three main stages which are shown in Figure 1. In the first stage, noise reduction technology is used to remove the noise and hairs in the skin cancer image; In the second stage, the color image is converted into a color space and adaptive color model is constructed; In the third stage, color information and distance histogram are used to extract the border of the lesions from the skin cancer image.
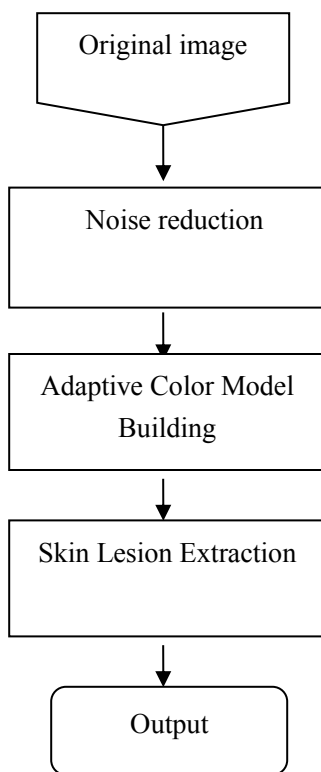
Figure1. System Architecture

2.2. Noise reduction

Because skin cancer images obtained generally include noise and hairs, thus noise reduction technology is used in the system so that the segmentation results will be good. In the past, a lot of techniques were developed for noise reduction. One of the techniques is Gaussian filter. Gaussian filter has many shortcomings. For example, Gaussian filter generally blurs the edges [27]. Thus, researchers tried to develop other noise reduction techniques such as bilateral filter for noise reduction. Let I(Y) be the original image and I(X) be filtered image, X and Y be the coordinates vectors, and σ be the standard deviation of the Gaussian distribution, then noise reduction using Gaussian filter can be expressed as [28][29][30]

$$I(X) = \frac{1}{2\pi\sigma^2} \cdot e^{-\frac{x^2+y^2}{2\sigma^2}} \cdot I(Y) \tag{1}$$

However, as I mentioned above, Gaussian filter generally blurs the edges of the images and thus bilateral filter is studied in this thesis. Different from Gaussian filter, bilateral filter show excellent performance in edge preservation while reducing the noise[31]. Since bilateral filter was proposed in [31], it has been applied to many noise reduction problems and is found effective.

Several types of bilateral filters [31][32] were developed in the past. One of them is Gaussian bilateral filter. Gaussian bilateral filter has the following format [31][33]

$$\bar{I}(X) = \frac{1}{C} \sum_{Y \in N(X)} e^{\frac{-\|Y-X\|^2}{2\sigma_d^2}} e^{\frac{-\|I(Y)-I(X)\|^2}{2\sigma_r^2}} I(Y) \qquad (2)$$

where $\bar{I}(X)$ is the pixel value for the output at location X, $I(Y)$ is the pixel value for the input at the location Y, X and Y are the two vectors composed coordinates. The two parameters: σ_d^2 and σ_r^2 can control spatial weights and intensity weights. And $N(X)$ is a neighborhood of $I(X)$, C is the constant normalization value:

$$C = \sum_{Y \in N(X)} e^{\frac{-\|Y-X\|^2}{2\sigma_d^2}} e^{\frac{-\|I(Y)-I(X)\|^2}{2\sigma_r^2}} \qquad (3)$$

2.3. Color Modeling

2.3.1. Color spaces

Several color spaces are investigated in this thesis. They are RGB, YUV, HSV , and YCbCr color space. YUV color space consists of two components: one is luminance (Y), which carries the brightness information of the images; the others are chrominance components U and V, which represent the color information of the images [34]. HSV color space uses two cylinders to represent the pixels in an RGB color space. In HSV color space, H means hue, which is the degree of the angle

11

around the center vertical axis in each cylinder; S means saturation, which indicates

the degree to which the hue differs from a neutral gray; V means value, which stands

for the illumination level [35]. YCbCr, Y′CbCr, or Y Pb/Cb Pr/Cr is the same color

spaces. Y is one component of this color space, and it means luminance. Cb and Cr

are the others, and they stands for blue and red difference [36]. The relationship

between RGB color space and other color spaces can be obtained by different

mathematics.

For RGB to YUV, the following equation is adopted

$$
\begin{aligned}
Y &= 0.299R + 0.587G + 0.114B \\
U &= -0.14713R - 0.28886G + 0.436B \\
V &= 0.615R - 0.51499G - 0.10001B
\end{aligned}
\tag{4}
$$

The conversion from RGB to YCbCr can be expressed as

$$
\begin{aligned}
Y &= 0.299R + 0.587G + 0.114B \\
Cb &= 0.564(B - Y) + 128 \\
Cr &= 0.713(R - Y) + 128
\end{aligned}
\tag{5}
$$

and the conversion from RGB to HSV can be obtained by

$$M = \max(R, G, B)$$
$$m = \min(R, G, B)$$
$$V = M / 255$$
$$S = \begin{cases} 1 - m/M & \text{if} \quad M > 0 \\ 0 & \text{if} \quad M = 0 \end{cases}$$
$$H = \begin{cases} \cos^{-1}\left[(R - 0.5G - 0.5B)/\sqrt{R^2 + G^2 + B^2 - RG - RB - GB} \right] & \text{if} \quad G \geq B \\ 360 - \cos^{-1}\left[(R - 0.5G - 0.5B)/\sqrt{R^2 + G^2 + B^2 - RG - RB - GB} \right] & \text{if} \quad G < B \end{cases}$$

……………………………………………………………………………………(6)

2.3.2. Adaptive Color Model Building

In order to use color information to detect the lesions, I need to build up the color model. In this thesis, I will investigate adaptive color modeling. My modeling is to build the color model for background and is composed of two steps. In the first step, I will build a general background color model for color detection. In the second step, when the general model is used to detect the color information in a specific image, I will use the color information from the four corners of the image detected by the general model to rebuild a color model specified for the image and then the new color model is used to detect the lesions in the image. Specifically, in the building processing, for each color space I will first calculate the mean and co-variance of color components using 20 images as the general color model. The following is an example of mean and co-variance computations in YUV color space.

13

$$M = (M_y, M_u, M_v) \tag{7}$$

$$C = \begin{pmatrix} C_{yu}(1,1) & C_{yu}(1,2) & C_{yv}(1,2) \\ C_{yu}(1,2) & C_{yu}(2,2) & C_{uv}(1,2) \\ C_{yv}(1,2) & C_{uv}(1,2) & C_{uv}(2,2) \end{pmatrix} \tag{8}$$

where M is the mean value and C is the co-variance. After the mean and co-variance of the general color model is built. When color detection begins for a specific image, the general color model is used to detect the color from four corners of the image. The color regions found using the general color model will be used to rebuild a color model for the specific image, which specific mean and co-variance are obtained for the image. About the specific color detection method, please refer to section 2.4.

Figure 2. Color Model Build

2.4. Skin lesion detection using distance histogram

The proposed lesion extraction is composed of three steps. They are skin color

detection, adaptive thresholding, and morphological post-processing.

2.4.1. Skin color detection

In this step, I will use color information to find the lesion regions. Based on the assumption that lesion regions and background have different color distributions, which can be characterized using mean and co-variance. Thus, I can classify a pixel as the part of background or the part of skin lesion using Mahalanobis distance

$$d(x,y) = \left(I(x,y) - M\right)^{T} \times C^{-1} \times \left(I(x,y) - M\right) \tag{9}$$

where *I(x,y)* is a vector constructed from the color components of pixel (*x,y*) and *d(x,y)* is the Mahalanobis distance at pixel (*x,y*). M and C are the mean and the co-variance of the adaptive color model obtained using equations (7) and (8). For each pixel in the original image I can obtain a *d(x,y)*. A pixel at location (*x,y*) is determined to be background by the following rules: for a pre-determined threshold *T*, if *d(x,y)<T*, then the pixel belongs to background regions, or it is classified into skin lesions. If I set the pixel values to be 1 if it is classified into skin lesion and to be 0 if it is classified into background, thus I obtain a binary image. For convenience, I denote the binary image by **B**, which has the same size as the original image.
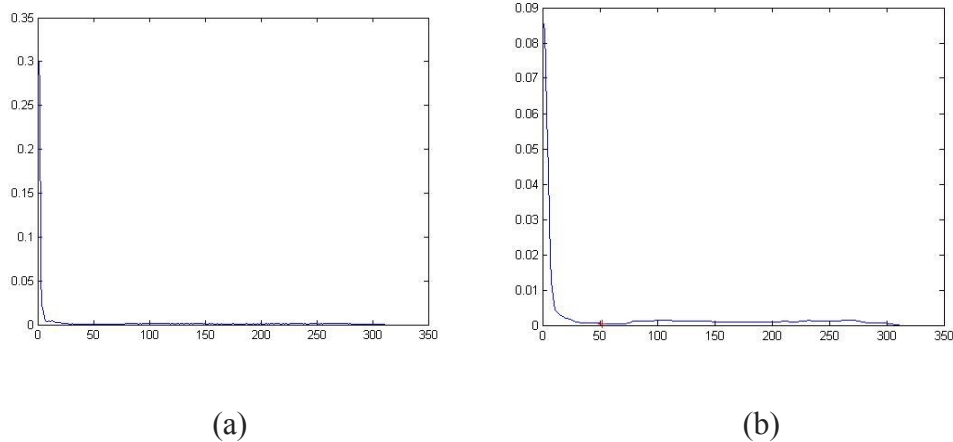
Figure 3. (a) Distance histogram without smoothing. (b) Smoothed histogram from (c). The red point is the threshold.

2.4.2. Adaptive Thresholding

The important steps to classify a pixel into skin lesions or background is the threshold *T*. Several methods have been proposed in different literatures. In this paper, I will develop a new adaptive thresholding method. The proposed method is distance histogram based method. The basic idea is to use $d(x,y)$ to generate a histogram and based on the histogram to determine the threshold **T**. However, the histogram generated directly from $d(x,y)$ is sticky and noisy, it is difficult to find the suitable T. In the proposed method, I first smooth the histogram directly obtained from $d(x,y)$ and the smoothed histogram will be used to get the threshold T. Figure 3 (a) shows the original histogram obtained directly from $d(x,y)$ and Figure 3 (b) shows the histogram smoothed using Gaussian filter(sigma=3). In order to find the

threshold T, I first find the lowest point between the first peak and the second peak of the smoothed histogram. The first peak stands for the number of the pixels which are closest to the adaptive color model (normal skin), so the lowest point splits the normal skin and the lesion skin. The parts whose distances are larger than the threshold are the lesion skin.

2.4.3. *Morphological processing*

In this step, morphological technology will be used. The image obtained using the method in section 2.3.2 may have noise in the normal skin and the lesion skin. I used two morphological operators to post-process the binary image **B.**

The first operator used is called connected-component labeling technology, which is used to remove the small objects. The basic idea of connected-component labeling technology is to separate the images into several objects and label them. During the processing, the background is labeled as 0, the first object is labeled 1, the second object is labeled as 2, and so on. After all the objects are labeled, I compare the size of these objects with a preset threshold. If the size of an object is smaller than the preset threshold, the object will be labeled as 0(the background). Figure 4(a) shows

the original binary image and Figure 4(b) shows the processed one.

(a)   (b)

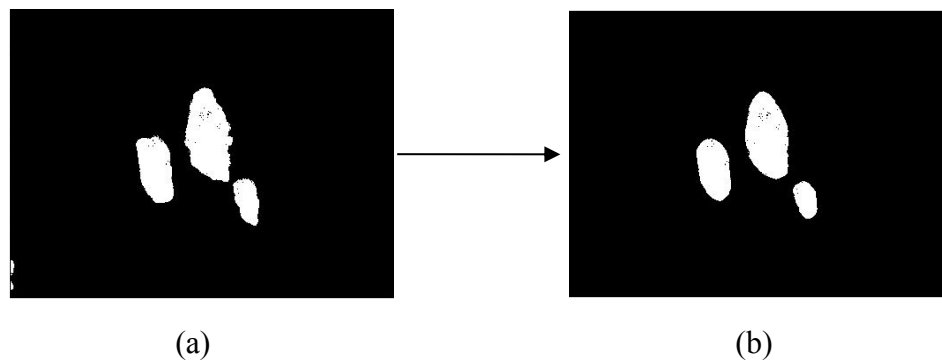**Figure 4.** (a) Original binary image; (b) Processed image

After the image is processed using the first morphological operator. The second operator used in the post-processing is closing operation. Closing operation can be done by dilation and erosion. It is useful to remove small holes. Figure 5 shows the images after closing operation.
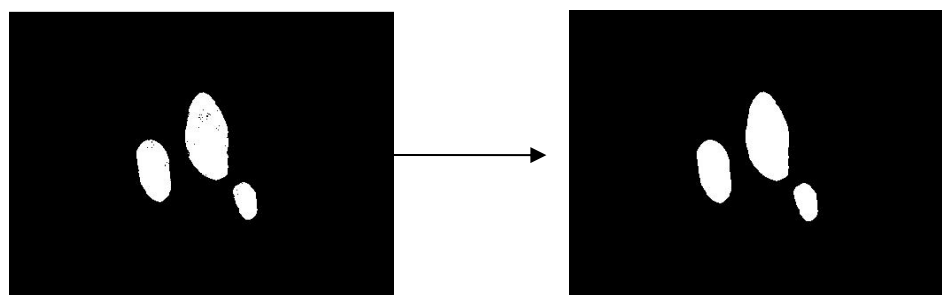

Figure 5. (a) Original binary image; (b) Processed image

2.5. Results and analysis

2.5.1 Noise Reduction on Synthetic Images

The first experiment was used to perform noise reduction on synthetic images. A red square image was created and different levels of noise were added to the image. In this thesis, Gaussian noise was added to the images. Figure 6 shows the original images and the corresponding images after noise reduction. In the figure, Column (a) lists the original synthetic images; column (b) lists the images after Gaussian noise with different variances are added; column (c) lists the filtered images obtained by Gaussian filter; column (d) lists the filtered images obtained by bilateral filter.

For evaluating the performance of the two filters, I used a quantitative measure which is mean square error (MSE) [37]. The MSE is defined as follows [37].

$$M = \sqrt{\sum_{(x,y)\in image}(I_0(x,y)-I(x,y))^2} \qquad (10)$$

$$MSE = (M_R + M_G + M_B)/3 \qquad (11)$$

where I_0 and I are the original synthetic image and the filtered image respectively. When noise reduction methods are compared, the smaller the MSE value is, the better the filtered result will be. Table 1 shows the comparison results of the two

noise reduction methods. From table 1, I can find that under different variances of Gaussian noise, the MSE values obtained by Bilateral filter are always smaller than the MSE values obtained by Gaussian filter. It means that Bilateral filter has a better performance than Gaussian filter when they are applied to reduce the noise in the synthetic images.

Table 1. MSE values obtained by Gaussian filter and Bilateral filter.

Variance	Gaussian filter (MSE)	Bilateral filter (MSE)
0.001	6.752	3.183
0.002	7.773	4.455
0.005	9.933	7.034
0.01	12.469	10.232
0.02	16.177	15.636

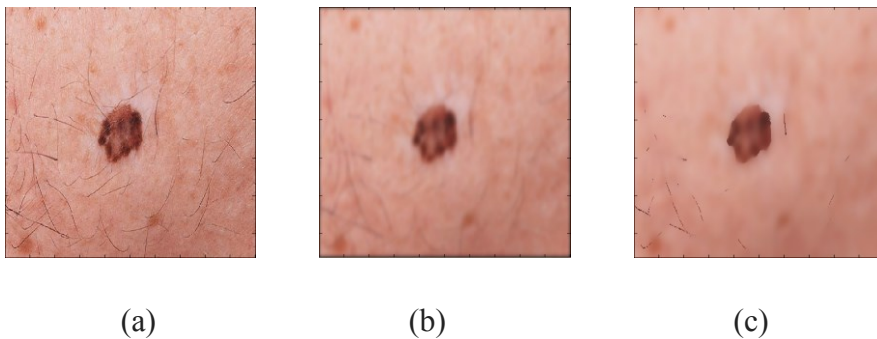(a)   (b)   (c)

Figure 6. (a) Original skin lesion image; (b) the image filtered by Gaussian filter; (c) the image filtered by bilateral filter.

2.5.2 Noise Reduction on Skin Lesion Images

How about the two filters work on the real images? In order to demonstrate the ability, I processed them on 20 different skin lesion images. Each image has one or more lesions, and some of them have hairs and noise. Figure 6 shows a sample of the original image and the corresponding image filtered by Gaussian filter and bilateral filter respectively. Figure 6.(a) shows the original skin lesion image, (b) shows the image filtered by Gaussian filter, and (c) shows the image filtered by bilateral filter. From Figure 6, I can find that bilateral filter is much better than Gaussian filter.

For evaluating the performance of the two filters working on the real images quantitatively, I need to evaluate two things. One is the performance for noise reduction, and the other is the performance for edge preservation. Because I focus on border detection, the performance of edge preservation is much more important. To evaluate the performance, I computed the local contrast of the edge region and homogeneous region. This measure can be expressed as

$$C_w(I) = \frac{1}{m}\sum_w |c(x,y)| \log(1 + |c(x,y)|) \tag{12}$$

where $c(x,y)$ is the local contrast at pixel (x,y) and can be expressed as

$$c(x,y) = 4I(x,y) - \{I(x-1,y) + I(x,y-1) + I(x+1,y) + I(x,y+1)\} \tag{13}$$

where $I(x,y)$ is the intensity for pixel (x,y) in an image, w is a set of edge points,

and m is the total number of the pixels in the edge points.

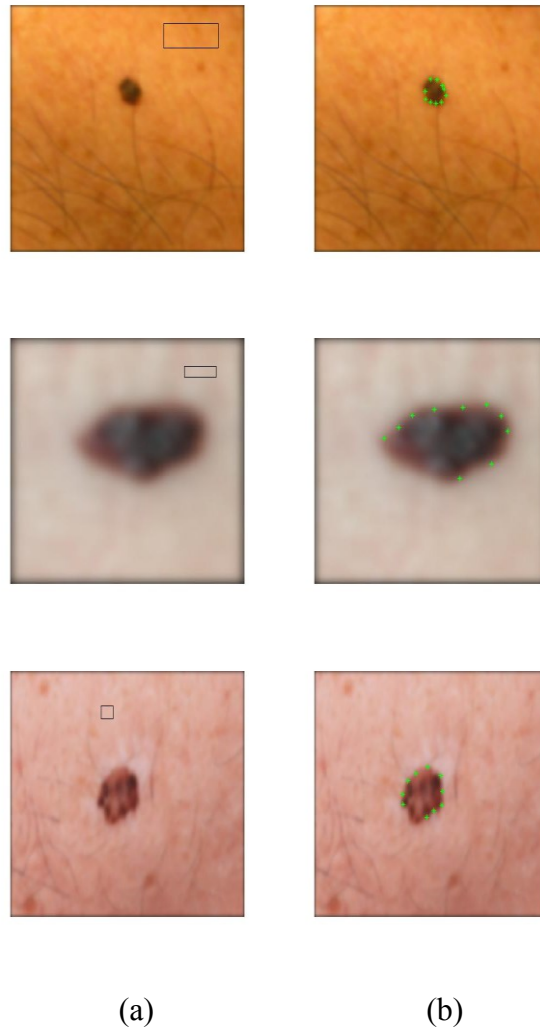(a)   (b)

Figure 7. Homogenous regions and edge points selected for evaluating the performance. From top to bottom, the images are labeled as image 1, image 2 and image3.

Three images were used to compare the performance of the two filtering methods.

For each image, I selected one homogenous region and one set of edge points for evaluation. Figure 7 shows the selections. Column **a** shows the homogenous regions selected and column **b** shows edge points set selected. When comparing the two filters, I consider the edge preservation in the set of edge points and noise reduction in homogenous regions selected. A good filter should remove the noise while preserving the edges in the image. Thus in the comparison of the two filters, I compared the edge preservation in the all edge points selected and made the selected homogenous have the

Table 2. The contrasts of selected homogenous regions

Image	Gaussian filter (C)	Bilateral filter (C)
Image 1	0.000016	0.000015
Image 2	0.000012	0.000011
Image 3	0.000196	0.000194

similar smoothness. Table 2 shows the average contrasts in the homogenous regions obtained by Gaussian filter and bilateral filter which corresponds to Figure 7(a). Table 3 shows the average contrasts in the all edge points obtained by Gaussian filter and bilateral filter respectively which correspond to Figure 7(b). From the two tables,

I can find that the contrast of the set edge points obtained by the bilateral filter is much bigger that those obtained by Gaussian filter while they have the similar contrast in the selected homogenous regions, which means that bilateral filter is much better than Gaussian filter.

Table 3. The contrasts of selected edge points set

Image	Gaussian filter (C)	Bilateral filter (C)
Image 1	0.0001	0.0004
Image 2	0.0002	0.0004
Image 3	0.0013	0.0035

2.5.3 Color Space Experiments

Experiments were performed to conform the proposed method work well. The experiments are divided into two parts. The first part is used to test the noise reduction method and the second part is used to test the proposed skin lesion extraction method.

$\sigma = 0.001$
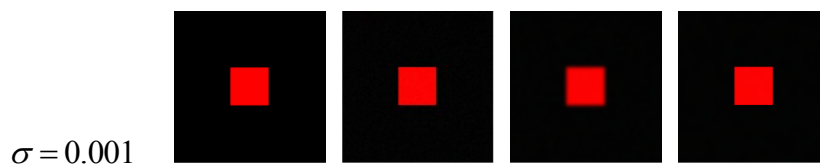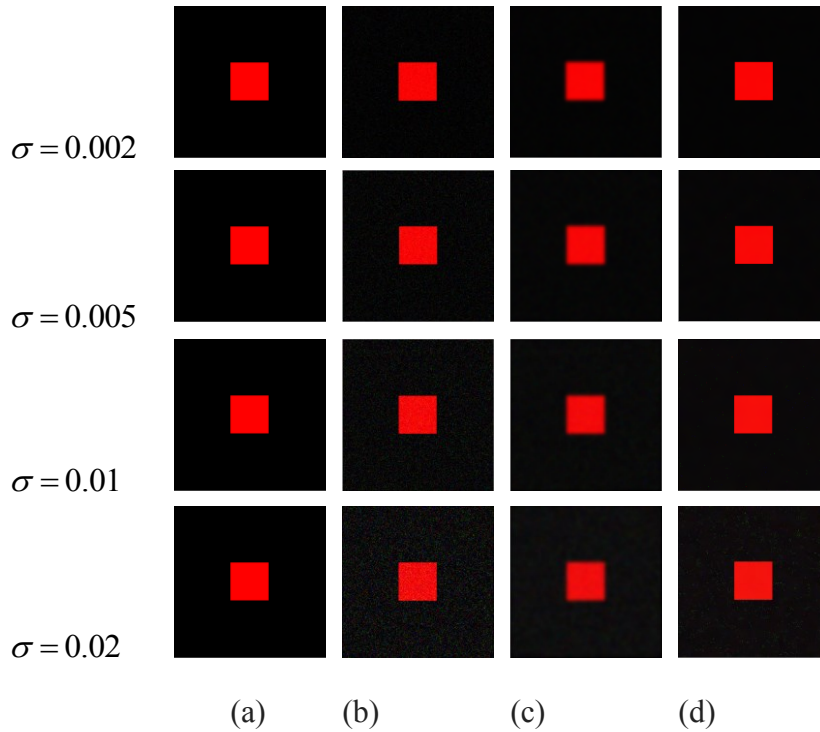
Figure 8. Filtered results of different Gaussian noised synthetic images. Column (a) is the original synthetic images; column (b) is the images after Gaussian noise with different variances are added; column (c) is the filtered images obtained by Gaussian filter; column (d) are the filtered images obtained by bilateral filter.

2.5.4 Experimental Results on Skin Lesion Segmentation

For skin lesion extraction, 20 images including one or more than one skin lesions were used in the experiments. Different color spaces were tested and compared. For each color space, the same procedure developed in Section 2.3 was used to extract skin lesions. Figure 9 shows some samples of lesion extraction using

different color spaces. From Figure 9, I can find that RGB, YUV and YCbCr color spaces almost achieved the same performance while HSV is much worse than the other three color spaces. To evaluate the performance for skin lesion extraction using different color spaces , Pratt's quality measurement metric (FOM) was used. The definition of the FOM is defined as:

$$F = \frac{\sum_{i=1}^{I_A} \frac{1}{1+\alpha(d(i)^2)}}{\mathbf{max}(I_A, I_I)} \tag{14}$$

where I_A and I_I are the number of boundary pixels which I_I is delineated by dermatologists and I_A is delineated by this system. $d(i)$ is the Euclidean distance between a pixel from I_I and the nearest pixel from I_A. α is a scaling constant (0.05 in my experiments). The best matching between the boundary segmented by CAD and by the technicians has F=1.

| a | b | c | d | e |
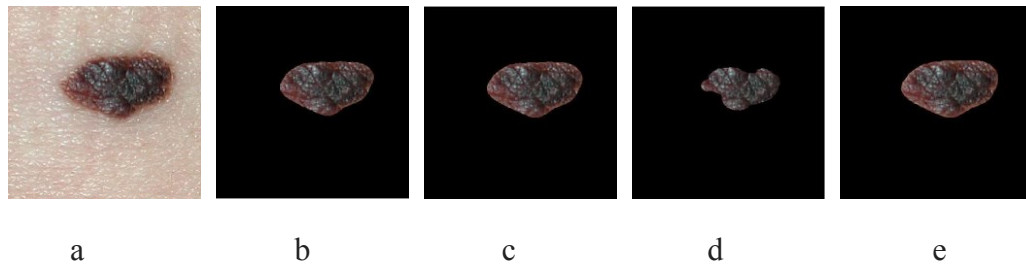
Figure 9. Segmentation results of skin lesions using 4 different color spaces. Column a: original skin lesion images, column; b: segmentation obtained by RGB color space; column c: segmentation obtained by YUV color space; column d:

Segmentation obtained by HSV color space; column e: segmentation obtained by YCbCr color space.

In experiments, one technician was used to segment the skin lesions manually and the results were used to compute FOMs using equation (13). Figure 10 shows the FOM values obtained using different color spaces. From Figure 10, I can find that YUV color space achieved the highest FOM values. So YUV color space performed better than other three color space using the proposed method.
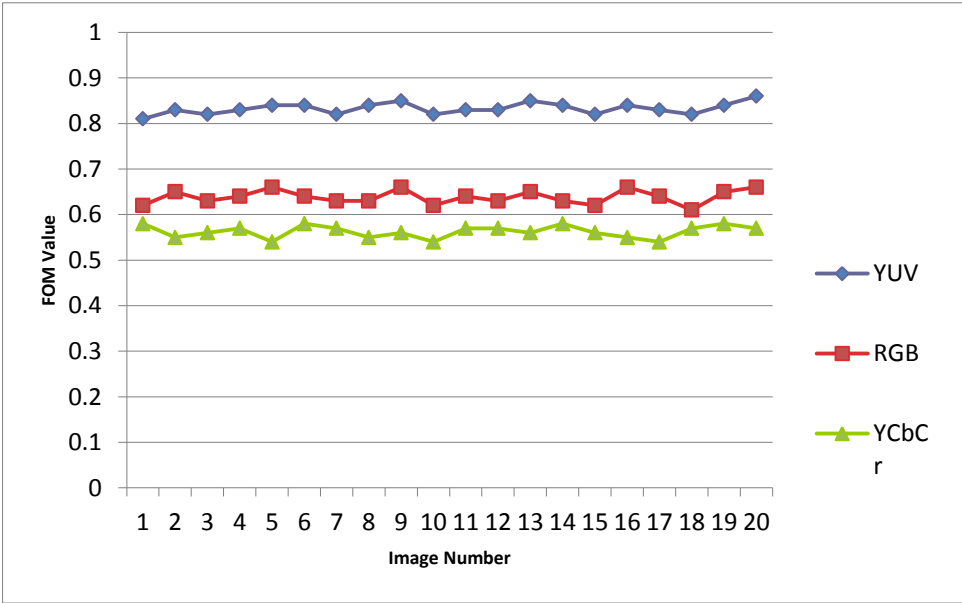
Figure 10. The FOM values of 20 segmentation images with RGB, YUV and YCbCr color spaces.

2.6. Speeding up with GPU

2.6.1 Introduction to GPU

In skin lesion boundary extraction, matrix operations are needed to be performed. Generally speaking, the computational cost will be very high when many matrix operations are involved. In order to speed-up the processing, I investigate GPU technology instead of CPU technology for matrix arithmetic in my skin lesion extraction algorithm. GPU is the abbreviation for Graphics Processing Unit and it is used to render videos [38]. GPU is highly optimized to perform advanced calculations such as floating-point arithmetic, matrix arithmetic and so on. The design of GPU is more of data processing than data caching and flow
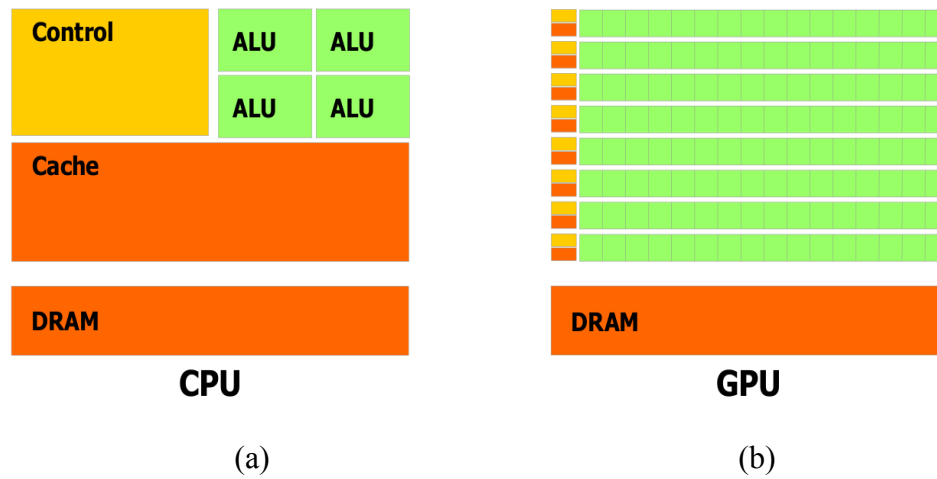
Figure 11. CPU and GPU structure

control than CPU [39]. The following graph (Figure 11 [39]) shows the difference between CPU and GPU in their structure. In CPU (see Fig.11 (a)), cache is designed for data caching; control is designed for flow control; ALU (Arithmetic Logic Unit) is designed for data processing. So the major difference between GPU and CPU is that GPU has highly parallel structure (much more ALUs) which makes it more effective than CPU for some operations.

2.6.2 Simulation

MATLAB provides GPU computing functionality which is well suited for a bunch of applications such as data analysis, signal processing, and image processing. Using the GPU functionality in MATLAB is much easier than using GPU computing technologies based on C or FORTRAN. Another advantage is that I don't need to know the libraries of GPU computing. I just need to be familiar with MATLAB language. In this thesis, I choose MATLAB to accelerate computation.

MATLAB has a certain Image Processing Toolbox function to process the images on GPU. The flow chart below is the main steps about how this function works.
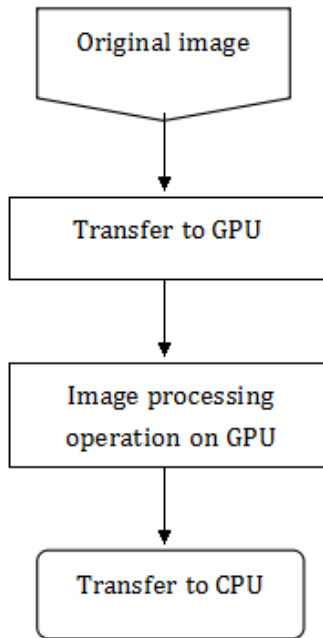
Figure 12. How GPU function works

Table 4: Hardware/Software Info

Entity	Specification
CPU	Intel Xeon Quad core @ 3.07 GHz
Installed Memory	16.00GB
System Type	64-bit
GPU	NVIDIA Quadro 600
Operating System	Windows 7
MATLAB Version	R2012b

In the processing, the first step is to transfer the data from CPU to GPU. At this step, MATLAB offers *gpuArray()* function to copy the numeric data to the GPU and return a gpuArray object. Any toolbox function that accepts a gpuArray as an input can work on the GPU. After processing, *gather()* function can be used to move the data back to the CPU from GPU.

In the following, I will provide an example of using GPU to solve 2-D cross correlation problem, which is shown in Figure 13. The specifications for experiments are listed in table 4. The MATLAB programs which use CPU and GPU to compute the cross correlation between matrix *a* and matrix *b* are shown in Figure 13 (a) and Figure 13(b) respectively. For comparison, I tried 5 different sizes (1000, 2000, 5000, 10000 and 120000) for matrix b to compare the performance between CPU and GPU. Figure 14 shows the execution time in different size of matrix b. When the size of matrix is 1000, the execution time is nearly the same. After that, the execution time of CPU grows rapidly. In contrast to CPU, the execution time of GPU grows slowly. While the size of matrix reaches 120000, the execution time of CPU is 7.4 times than GPU. In a conclusion, the bigger the size of matrix is, the better the GPU will perform.

```
sizes=[1000,2000,5000,10000,120000];       sizes=[1000,2000,5000,10000,120000];
%return a matrix of 100 x 100             %return a matrix of 100 x 100
a=rand(100);                              a=rand(100);
cpuTime=zeros(size(sizes));               gpuTime=zeros(size(sizes));
for s=1:numel(sizes)                      for s=1:numel(sizes)
    b=rand(sizes(s));                         b=rand(sizes(s));
    %xcorr2                                   %xcorr2 on gpu
    st=tic;                                   gst=tic;
    c=xcorr2(a,b);                            ga=gpuArray(a);
    cpuTime(s)=toc(st);                       gb=gpuArray(b);
end                                           gc=xcorr2(ga,gb);
                                              gres=gather(gc);
                                              gpuTime(s)=toc(gst);
                                          end
```

            (a)   (b)

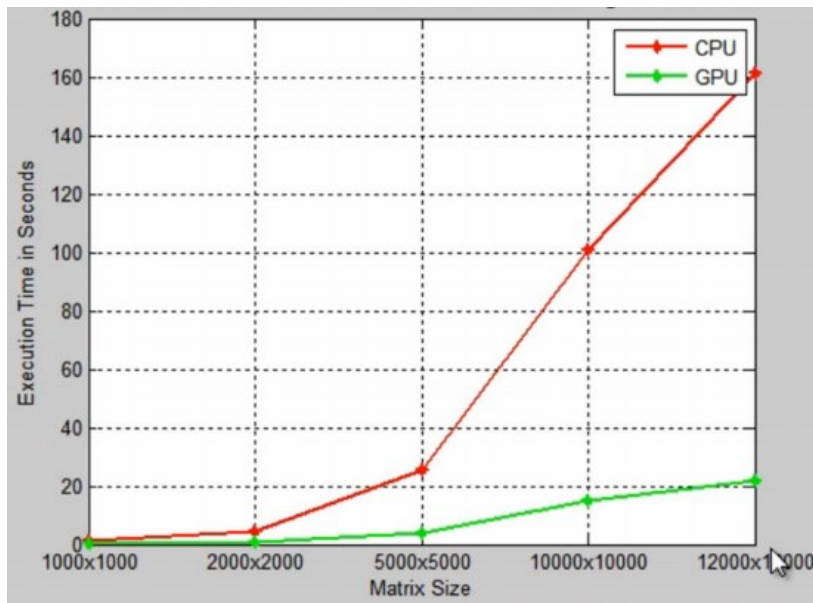**Figure 13.** 2-D Cross Correlation Example

Figure 14. CPU vs GPU Cross-Correlation of 2-D Data

2.6.3. Skin lesion detection using GPU technology

In matrix operations, the size of the matrix will affect the performance. There is a

threshold for you decide to use GPU or not. If the matrix size is below this threshold,

the computing speed between CPU and GPU are nearly the same. Otherwise, GPU is

faster than CPU. The bigger the matrix size is, the faster the GPU will be. In my skin

lesion extraction, I used GPU technology to perform the matrix operations in

equation (8), and the results are shown above Fig.15. From Figure 15, I can find that

border extraction involving GPU technology can improve from 30% to 40% in

running speed according to the matrix size.
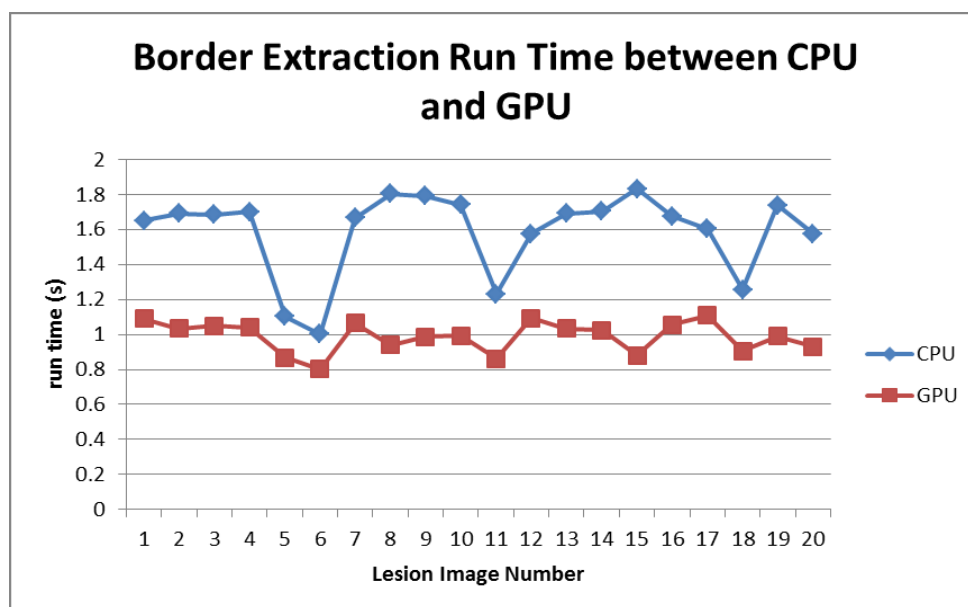
Figure 15. Comparison of CPU and GPU technologies for border extraction

Although the GPU can only improve 30%~40% in computational cost, the GPU has

potential application in skin lesion extraction when all-body skin image are available.

In this case, the size of the image will be very big and computation technology based on CPU technology cannot satisfy the applications. Besides, in my application, I did use specific outside GPU, I used the GPU coming with the computer. If specific outside GPU is used, the computation cost will be increased a lot. I plan to investigate this issue in the future.

Chapter 3. An Iphone Mobile Application for Aiding Skin Cancer Diagnosis

3.1. Introduction

A smartphone is an advanced mobile phone that is built on a mobile operating system (OS) with much more powerful computing capability than feature mobile phones [40]. Many smartphones usually have one or more powerful processors, large memory, and storage capability. Besides these core components, most of smartphones are equipped with a variety of sensors and accessories which allow them to interact with the environment easily. These components include high-megapixel cameras, high-resolution touchscreen, GPS navigation unit, Wi-Fi, mobile broadband, and so on. [41]. Because of these great features, many applications based on smart phone have been become possible. In fact, currently applications based on smartphones are becoming great demands in my society and many applications are based on smartphones, such as visual recognition, security, medical applications, and so on.

A mobile application (mobile app) is a kind of software applications running on mobile phone. In the older generations of mobile phones, mobile apps were

developed to provide some simpler functionality such as calendar, maps, clock, and weather information. With the new generations of mobile phone, such as smartphones, coming out, mobile app developers started to turn their attentions into other categories of applications, such as music playing, mobile games, mobile chatting, ticket purchase, and so on [42]. Health application running on smartphones is one of the big research areas. In the past, some work has been done in this area. In [43], Wadhawan developed a portable library to detect skin cancer automatically. This library can be used on smartphones (iPhone 4), and but the performance in real applications is not good. In [44], Li developed a mobile application based on the interaction physical-activity housekeeper (IPHA), which contributes to monitoring the physical status of the elder people. In [45], the authors proposed an ambulatory electrocardiographic monitoring application, and the application is based on iOS and Android system. In [46], Kong proposed an automatic camera phone based multi-view food classification application. The purpose of this application is to evaluate food intake automatically using food recognition from images. This application has been implemented on iPhone, and the recognition accuracy is about 84% for common food items. In [47], the authors present a health management application implemented on iPhone, and it uses QR-code to input food information such as nutrition and calorie. The application can provide diet recommendations to

the users. In [48], Chemlal developed a real time prediction system for blood glucose running on iPhone. The purpose of this application is to monitor physical activities of the users with type 2 diabetes. Gegg-Harrison in [49] proposed a new application of smartphones to make the Lung Cancer Survivability Prediction Tool more accessible and convenient to doctors. In [50], Chan developed an application using the capabilities of the accelerometer within the iPhone to identify the users' walk along a flat surface. The aim of the application is help elder people avoid injury from falling.

In this thesis, a mobile based skin cancer diagnosis application is developed. In this application, the user with an iPhone installed with the proposed application can use the iPhone as a diagnosis tool to find the potential skin lesions in a persons' skin and compare the skin lesions detected by the iPhone with the skin lesions stored in a database in a remote server.

3.2. Development Environment and System Structure

In order to develop the application for aiding skin cancer diagnosis, one of the first things is to select development platform. Based on the difficulty of development and market share, I decided to develop my applications on iOS platform. iOS uses Xcode

development environment which can run on Apple Mac Machine. Xcode was first released in 2003, and it was devised for developing software for OS X and iOS [51]. The strength of the iOS platform is that it has much fewer releases than other platforms, and Apple supports all of these releases.

The second thing to develop the application is to select a language which can be supported by IOS platform. Objective-C programming language is the most supported programming language in IOS platform [52] and thus I select it as the language to write the codes.

For the reason above, I chose Xcode 5.0 as my development environment and Objective-C as my programming language to develop my iOS app.

3.3. Skin cancer Image retrieval using boundary information

3.3.1 Introduction to Image Retrieval

Searching and retrieving images is the main task for the image retrieval system. One of important research area is content based image retrieval. The basic idea of content based image retrieval is to use image to find images. Features such as color, texture, shape and other information are extracted from the query image and then the features

are compared with the features of the images in the database. A similarity metric is used to compare the similarity if the images. Some work has been done in the past. In [53], Krishnapuram proposed a fuzzy image retrieval system. This system used fuzzy set theory and the experimental results shows that it is possible to improve the performance of content-based image retrieval by using fuzzy set theory. In [54], Suzuki designed a new image retrieval system on multimedia networks in 2000, and the system uses a sketched image to retrieve similar images. In 2003, Stejic Z. proposed a relevance feedback-based image retrieval system which the users can select regions and features, and it brought average 6%-30% increase in retrieval precision [55]. In [56], Yang presented a boosting framework for distance metric learning method for medical image retrieval and the authors declared that their framework worked well for regular image data sets with less computational complexity. In [57], Kotoulas introduced an image retrieval algorithm based on composite color image histogram. The algorithm is faster and can achieve higher retrieval accuracy than some traditional histogram based image retrieval. In many image retrieval systems, one problem is that the retrieval accuracy may vary on different queries. For tackling this problem, Li [58] proposed a query difficulty guided image retrieval system. This system can estimate the queries' performance by different difficulty degrees, and use the optimization approaches to retrieve the

image and thus obtain high accuracy.   Existing texture image retrieval systems have the following shortcomings: low retrieval accuracy and high computational cost. Kokare [59] proposed a novel approach to attack this problem. In the proposed approach, he used a set of dual-tree rotated complex wavelet filter and dual-tree-complex wavelet transform jointly to obtain the features of texture. The retrieval rate was improved from 69.61% to 77.75%. Besides using global features to retrieve images, other research work uses local features to retrieve images. The authors in [60] proposed segmentation based image retrieval system. In the system, an image is segmented into different regions and the image retrieval is performed on the region level.

In this thesis, I will study skin lesion image retrieval. My aim is to find the cases with similar shapes in the database so that a user can analyze the possibility that a skin lesion is malignant. The feature used in the thesis is boundary information - the shape of the skin lesion. Based on research, shape of the skin lesion can tell whether a skin lesion is benign or malignant. In order to compare the similarity of the shapes, Fourier descriptor is used to extract the shape feature.

3.3.2 Feature Extraction Using Fourier Descriptor

Fourier descriptor is a way of encoding the shape of a 2-D object, object recognition and boundary shape representation are two main applications with Fourier Descriptors. The second application is always used for shape matching. The Fourier descriptor of a shape can be calculated as: First, find the coordinates of all points on the skin lesion boundary and put them in a $set(x_k, y_k)(k = 0,1,...N)$. Here N indicates how many number of the points on the boundary. Then a complex vector is created using the coordinates above. The typical way is to change the name of the x axis to R for "real", and the y axis to I for "imaginary" as follows

$$s(k) = x_k + iy_k \tag{15}$$

After creating the complex vectors $s(k)$, discrete Fourier Transform is performed on the set $s(k)$

$$F(u) = \frac{1}{N}\sum_{k=0}^{N-1} s(k)e^{-i2\pi u/N} \tag{16}$$

where $u = 0, 1, ..., N - 1$. The complex coefficients F(u) are called the Fourier descriptor of the boundary.

3.3.3. Similarity Metric

In order to compare the similarity between two boundaries, I need to develop a similarity metric. I will use the magnitude of the Fourier coefficients to compare two shapes. Let $F_Q(u)$ and $F_D(u)$ represent the coefficients of the query shape and an shape in the database. The similarity between shapes D_s of these two components is

computed by

$$D_S = \sqrt{\sum_u (F_Q(u) - F_D(u))^2} \tag{16}$$

3.4. System description

3.4.1. Flowchart for the IPhone application prototype

The iPhone application includes two parts: the skin lesion image collection parts and the image retrieval part. The skin lesion image collection part permits the users to upload skin lesion images into the server. After the server receives the images, it will send E-mail to the administrator and the administrator will determine whether the images will be collected into the server.
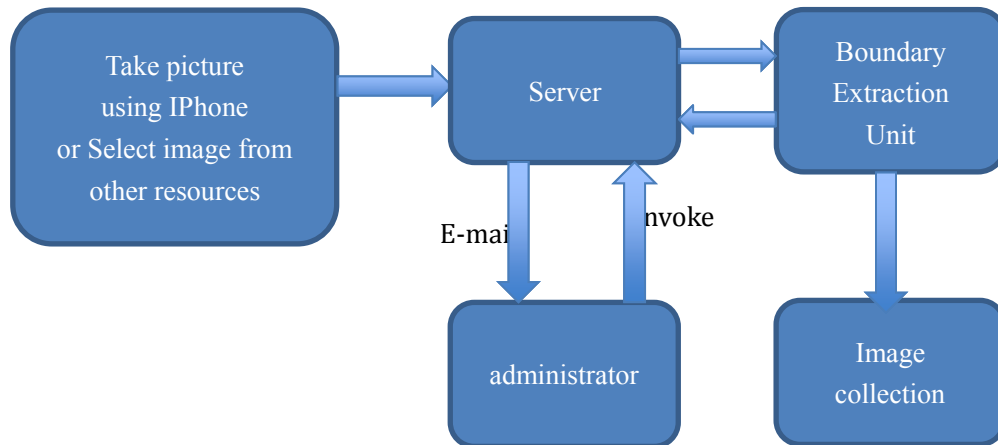

Figure 16. Skin lesion image collection part

After the administrator decides to collect an image into the server, the image will be sent to boundary extraction unit and the boundary of the skin lesion will be extracted. After the boundary information is extracted, the image and the extract boundary

information will be sent to the server for storage. Figure 16 shows how flow chart of the first part.

The second part of the application is image retrieval part. In this part, a user can take a picture using his iPhone and use the acquired picture as the query image. The query image will be sent to the sever side and the image will be processed by the image retrieval unit. The image retrieval unit will extract the boundary of the skin lesion and compare the similarity between the query image and the images stored in the server. The image retrieval unit will rank the image based on the similarity computed using equation (16), 3 mostly matched skin lesion image will be returned. Figure 17 show the flow chart of image retrieval part.
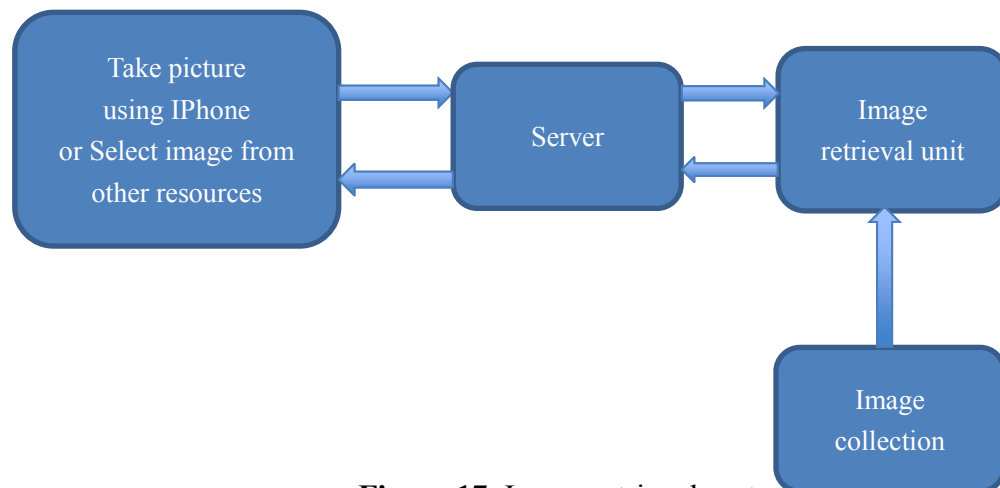

Figure 17. Image retrieval part

3.4.2. Interface for IPhone Application

My iPhone application is designed to be easy using for users. The uses can click the app to launch the application. Figure 18 shows the main storyboard of the application.

After a user clicks the SkinLesion button, there are two choices. One is for the users which can use for retrieving images from the server and the other button is used for upload and retrieval. The first choice is designed for patients(retrieval button) and the second choice is designed for doctors(retrieval and upload button). In the first choice, the users can just use image to retrieve similar images from the server while the users can retrieve and upload skin lesion images in the second choice. For uploading an image, the users need to take a photo using the phone's camera or choose a photo in phone's library. This can be done by click the "Choose Image" button. When the photos are prepared, the users can click the "Send" or "Upload" button. Then an email sending interface will appear, and the users just need to click the "send" button because the email has been atomically filled by my system. The email will be sent to the server administrators, and an administrator will invoke the processing of the image on the server part and return the results back. The "retrieval" button is used to get the results.
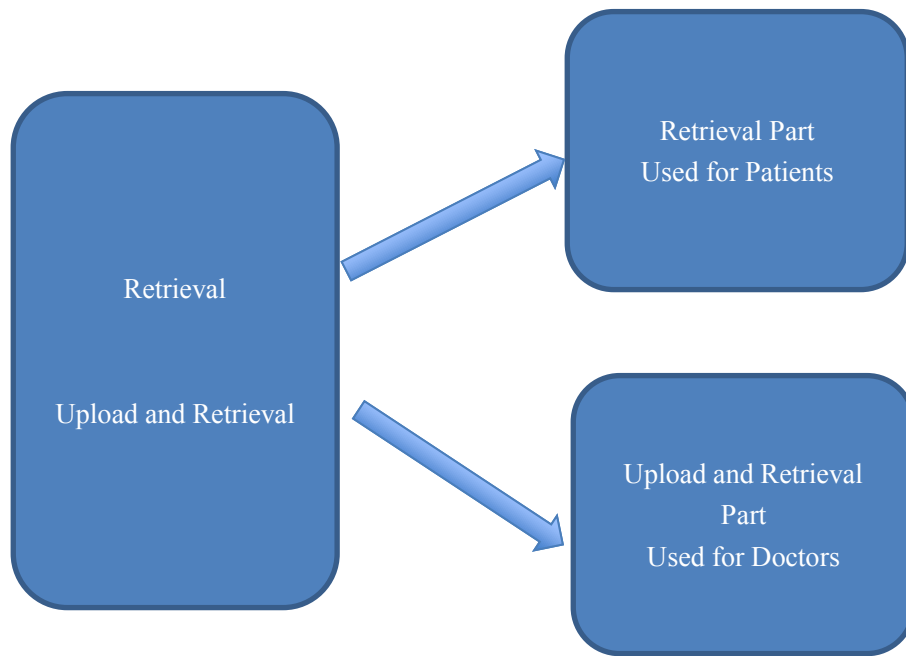
Figure 18. Main storyboard

3.5. Experimental Results

There are 50 skin cancer images in my collection. Mostly of them are from No1. Suzhou Hospital and the rest are from the Internet. Each of them has been segmented and the boundary information has been recorded. In the following, I present some of the image retrieval results using different query images. The retrieval is performed as follows: the user will upload an image and send it to the server. The server will compute the similarity between the query image and the images in the collection in the server side. The mostly matched 3 image will be returned and send back to the

user.

In Figure 21, (a) is the query image, and (b) to (d) are the retrieval results, I rank them descending by D_s. From the figure, I can find that the retrieval results are good. Figure 22 shows the retrieval result using another image as query image.
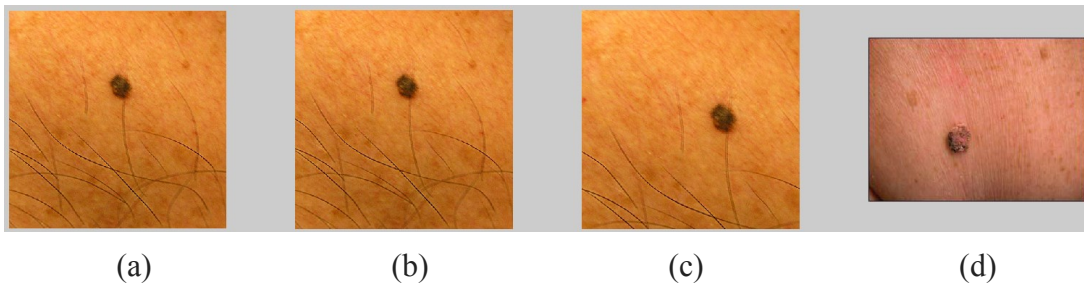

| (a) | (b) | (c) | (d) |

Figure 19. (a) is the query image, (b) to (d) are the retrieved images
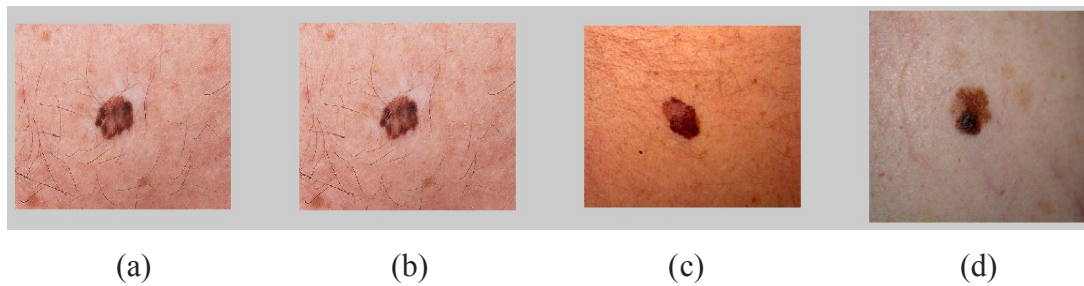

| (a) | (b) | (c) | (d) |

Figure 20. (a) is the query image, (b) to (d) are the retrieved images

Chapter 4. Summary and Future work

In this thesis, skin lesion segmentation is investigated and a new skin border extraction based on distance histogram and color information is proposed. The new distance histogram based skin lesion border extraction can achieve high accuracy.

In order to remove the noise, two noise reduction technologies were investigated. Gaussian filter and bilateral filter were compared in the noise reduction part. The experimental results show that bilateral filter is better at edge preservation than Gaussian filter.

I also compared four color spaces (RGB, YUV, HSV and YCbCr) for skin lesion extraction, and I found that YUV color space is more suitable for the proposed method. Because YUV color space separately stores the brightness information (Y) and chrominance information (UV) of images, it can reduce the effect by brightness for color images.

In order to improve computation efficiency, GPU techniques for skin lesion extraction is investigated and the results show GPU has potential applications in skin

lesion extraction.

Based on my skin lesion extraction system, an iPhone application for skin lesion image retrieval system is developed. In the proposed system, Fourier Descriptor is used to extract features and the magnitude of the Fourier coefficients is used for shape matching. Experimental results show the potential of the proposed image retrieval system.

Besides boundary information, other information such as the texture information, color information is also useful in skin cancer diagnosis. Thus I plan to integrate this information into the system for skin cancer diagnosis in the future.

References

1. Cancer Research UK, "Cancer Worldwide – the global picture", http://www.cancerresearchuk.org/cancer-info/cancerstats/world/the-global-picture/, Sept. 2012.

2. World Health Organization, http://www.who.int/en/.

3. Science Daily, "Cancer Projected To Become Leading Cause Of Death Worldwide In 2010", http://www.sciencedaily.com/releases/2008/12/081209111516.htm, Dec 2008.

4. Skin Cancer Foundation, "Skin Cancer Facts", http://www.skincancer.org/skin-cancer-information/skin-cancer-facts.

5. National Cancer Institute, "Common Cancer Type", http://www.cancer.gov/cancertopics/types/commoncancers, Jan 2013.

6. Centers for Disease Control, "Skin cancer," http://www.cdc.gov/cancer/ skin/ (May 8, 2013).

7. American Academy of Dermatology, "Skin Cancer", http://www.aad.org/media-resources/stats-and-facts/conditions/skin-cancer.

8. Robert S. Porter, "The Merck Manual", July 20, 2011. & D. L. Kasper, E. Braunwald, and A. Fauci, "Harrison's Principles of Internal Medicine", 17th ed., McGraw-Hill, New York (2008). (put 6 and 7 together)

9. R. Anderson, A. Parrish, "The optics of human skin", The Journal of Investigative Dermatology, Vol. 77, pp 13-19, 1981.

10. T. DiChiara. "Pictures of Moles and Melanoma skin cancer – Learn o tell the difference with pictures.", Sept. 2010.

11. Sun Protection and Products Guide, "Learning the ABCDE rule for skin cancer can save your life!", http://www.sun-protection-and-products-guide.com/ABCDE-rule-for-skin-ca

ncer.html.

12. American Cancer Society, "How is lymphoma of the skin diagnosed", http://www.cancer.org/cancer/lymphomaoftheskin/detailedguide/lymphoma-of-the-skin-diagnosed, March 2013.

13. Kunio Doi, "Computer-Aided Diagnosis in Medical Imaging: Historical Review, Current Status and Future Potential". Computer Med Imaging Graph, Vol. 31, pp 198-211, 2007.

14. F. Ercal, A. Chawla, W. V. Stoecker, H. C. Lee, and R. H. Moss, "Neural network diagnosis of malignant melanoma from color images," IEEE Trans. Biomed. Eng. 41(9), 837–845 (1994).

15. Opticom Data Research, "MoleSense - Take Control of Your Mole", http://www.opticomdataresearch.com/molesense.htm

16. H. Ganster, "Automated Melanoma Recognition", IEEE Trans. Medical Imaging. 20(3), (2001)

17. Fotofinderin, http://www.handyscope.net/

18. J. Tang, "A multi-direction GVF snake for the segmentation of skin cancer images," Pattern Recognition 42(6), 1172–1179 (2009).

19. J. E. Golston, W. V. Stoecker, R. H. Moss, and I. P. S. Dhillon, "Automatic detection of irregular borders in melanoma and other skin tumors," Comp. Med. Imaging Graphics 16(3), 199–203 (1992).

20. J. E. Golston, R. H. Moss, and W. V. Stoecker, "Boundary detection in skin tumor images: An overall approach and a radial search algorithm," Pattern Recognition 23(11), 1235–1247 (1990).

21. Q. Abbas, I. Fondón, and M. Rashid, "Unsupervised skin lesions border detection via two-dimensional image analysis," Comp. Methods Programs Biomed. 104(3), e1–e15 (2011).

22. S. E. Umbaugh, R. H. Moss, and W. V. Stoecker, "An automatic color segmentation algorithm with application to identification of skin tumor

borders," Comp. Med. Imaging Graphics 16(3), 227–235 (1992).

23. G. Schaefer, M. I. Rajab, M. E. Celebi, and H. Iyatomi, "Colour and contrast enhancement for improved skin lesion segmentation," Comp. Med. Imaging Graphics 35(2), 99–104 (2011).

24. X. Yuan, N. Situ, and G. Zouridakis, "Automatic segmentation of skin lesion images using evolution strategies," Biomed. Signal Process. Control 3, 220–228 (2008).

25. X. Yuan, N. Situ, and G. Zouridakis, "A narrow band graph partitioning method for skin lesion segmentation," Pattern Recognition 42(6), 1017–1028 (2009).

26. L. Xu et al., "Segmentation of skin cancer images," Image Vision Comp. 17(1), 65–74 (1999).

27. Kim, H.K., "Filtering in the time and frequency domains", IEEE, Vol 66, pp 360, 1978

28. R.A. Haddad and A.N. Akansu, "A Class of Fast Gaussian Binomial Filters for Speech and Image Processing," IEEE Transactions on Acoustics, Speech and Signal Processing, vol. 39, pp 723-727, March 1991.

29. Shapiro, L. G. & Stockman, G. C: "Computer Vision", page 137, 150. Prentence Hall, 2001

30. Mark S. Nixon and Alberto S. Aguado. Feature Extraction and Image Processing. Academic Press, 2008, p. 88.

31. C. Tomasi and R. Manduchi, "Bilateral Filtering for Gray and Color Images," Proc. IEEE ICCV 1998, 839–846 (1998).

32. I. Butt and N. Rajpoot, "Multilateral Filtering: A Novel Framework for Generic Similarity-based Image Denoising," Proc. IEEE ICIP 2009, 2981–2984 (2009).

33. M. Zhang, "Bilateral Filter in Image Processing," Master's Thesis, Louisiana State University, Baton Rouge, LA (2009).

34. N. Vandenbroucke, L. Macaire, and J. Postaire, "Color image segmenta- tion by pixel classification in an adapted hybrid color space: application to soccer image analysis," Comp. Vision Image Understanding 90(2), 190–216 (2003).

35. J. L. Liu and D. G. Kong, "Image retrieval based on weighted blocks and color feature in: International Conference on Mechatronic Science," Proc. Int. Conf. Mechatronic Sci. Electric Eng. Comp., Jilin, China, 921–924 (2011).

36. H. Noda and M. Niimi, "Colorization in YCbCr color space and its application to JPEG images," Pattern Recognition 40(12), 3714–3720 (2007).

37. S. H.-S. Hung, "Lower bound on average mean-square error for image restoration," IEEE Trans. Signal Process. 39(2), 497–499 (1991).

38. M. B. Kolund!zija and P. D. Zoric, "Efficient evaluation of MoM matrix elements using CPU and/or GPU," Proc. IEEE EUCAP 2012, 702–706 (2012).

39. NVIDA CUDA, "Non-graphic computing with graphics processors," http://ixbtlabs.com/articles3/video/cuda-1-p1.html (Oct, 21, 2008).

40. Nusca, A., "Smartphone vs. feature phone arms race heats up; which did you buy?",
<http://www.zdnet.com/blog/gadgetreviews/smartphone-vs-feature-phone-arms-race-heats-up-which-did-you-buy/6836> (Aug, 20, 2009)

41. Karagyris, A., Karagyris, O.,Pantelopoulos, A., "DERMA/Care: An Advanced image-Processing Mobile Application for Monitoring Skin Cancer", Proceedings of   IEEE 24th International Conference on Tools with Artificial Intelligence (ICTAI), pp 1-7, 2012, Athens.

42. Pogue, David, "A Place to Put Your Apps". New York Times, Jan 2013.

43. Wadhawan, T., Situ, N., Lancaster, K., Yuan, X. Zoridakis, G., "SkinScan: A portable library for melanoma detection on handheld devices", Proceedings of IEEE International Symposium on Biomedical Imaging: From Nano to Macro, pp 133-136, March 2011, Chicago, IL.

44. Lin, C., Wang, C., Chen, J., etc,   "Interaction Physical-Activity Housekeeper for Silver-Haired Citizen Using Wireless Sensor and Mobile Healthcare iPhone", Proceedings of IEEE 37th Annual on Computer Software and Applications Conference,   pp 274-275, July 2013, Kyoto.

45. Saldarriaga, A.J., Perez, J.J., Restrepo, J., Bustamante, J.,   "A mobile application for ambulatory electrocardiographic monitoring in clinical and domestic environments", Proceedings of Pan American on Health Care Exchanges, pp 1-4, April 2013, Medellin.

46. Kong, F., Tan, J., "DietCam: Regular Shape Food Recognition with a Camera Phone", Proceedings of International Conference on Body Sensor Networks (BSN), pp 127-132, May 2011, Dallas, TX.

47. Hsu H., Chang M., Yen, N.Y., "A health management application with QR-Code input and rule inference", Proceedings of   International Conference on Information Security and Intelligence Control (ISIC), pp 119-122, Aug. 2012, Yunlin.

48. Chemlal, S., Colberg, S., Satin-Smith, M., Gyuricsko, E., etc, "Blood glucose individualized prediction for type 2 diabetes using iPhone application", Proceedings of   IEEE 37th Annual Northeast on Bioengineering Conference (NEBEC), pp. 1-2, April 2011, Troy, NY.

49. Gegg-Harrison, T., Zhang, M., Meng, N, Sun, Z., Yang, P., "Porting a cancer treatment prediction to a mobile device", Proceedings of Annual International Conference of the IEEE on Engineering in Medicine and Biology Society, pp 6218-6221, Sept. 2009, Minneapolis, MN.

50. Chan, H.K.Y., Zheng, H., Wang H., Gawley, R., etc, "Feasibility study on iPhone accelerometer for gait detection", Proceedings of 5th International Conference on Pervasive Computing Technologies for Healthcare (PervasiveHealth), pp 184-187, May 2011, Dublin.

51. Apple Inc., "Xcode on the Mac App Store", Oct 2012.

52. Simon, B., "DID APPLE MAKE A MISTAKE CHOOSING OBJECTIVE-C

FOR IPHONE SDK?", Simon Brocklehurst's Technology Blog, May 2010.

53. Krishnapuram, R., Medasani, S., Jung, S., Choi, Y., Balasubramaniam, R., "Content-based image retrieval based on a fuzzy approach", IEEE Transactions on Knowledge and Data Engineering, Vol. 16, No. 10, pp 1185-1199, Oct. 2004.

54. Suzuki, K., Nagao, M., "Image retrieval using sketched image on multimedia networks: new criteria for designing new type of TV sets", IEEE Transactions on Consumer Electronics, Vol. 6, No. 1, pp 227-236, Feb 2000.

55. Stejic, Z., Takama, Y., Hirota, K., "Relevance feedback-based image retrieval interface incorporating region and feature saliency patterns as visualizable image similarity criteria", IEEE Transactions on Industrial Electronics, Vol. 50, No. 5, pp 839-852, Oct 2003.

56. Yang, L., Jin, R., Mummert, L., Sukthankar, R., etc, "A Boosting Framework for Visuality-Preserving Distance Metric Learning and Its Application to Medical Image Retrieval", IEEE Transactions on Pattern Analysis and Machine Intelligence, Vol. 32, No. 1, pp 30-44, Jan 2010.

57. Kotoulas, L., Andreadis, I., "Colour histogram content-based image retrieval and hardware implementation", IEEE Proceedings on Circuits, Devices and Systems, Vol. 150, No. 5, Oct. 2003.

58. Li, Y., Geng, B., Tao, D., Zha, Z., Yang, L., Xu, C., "Difficulty Guided Image Retrieval Using Linear Multiple Feature Embedding", IEEE Transactions on Multimedia, Vol. 14, No. 6, pp 1618-1630, Dec. 2012.

59. Kokare, M, Biswas, P.K., Chatterji, B.M., "Texture image retrieval using new rotated complex wavelet filters", IEEE Transactions on Systems, Man, and Cybernetics, Part B: Cybernetics, Vol. 35, No. 6, pp 1168-1178, Dec 2005.

60. Avula S. R., Tang J., Acton S., "An object-based image retrieval system for digital libraries", Multimedia Systems Journal, vol.11, No. 3, pp. 2006.